

A model of smooth pursuit in primates based on learning the target dynamics

Tomohiro Shibata^{a,b,c,*}, Hiromitsu Tabata^d, Stefan Schaal^{b,e}, Mitsuo Kawato^b

^a*Metalearning and Neuromodulation, CREST, Japan Science and Technology Corporation, Kyoto, Japan*

^b*ATR Computational Neuroscience Labs, Kyoto, Japan*

^c*Graduate School of Information Science, Nara Institute of Science and Technology, Nara 630-0192, Japan*

^d*Graduate School of Medicine, Kyoto University, Kyoto, Japan*

^e*Computer Science and Neuroscience, University of Southern California, LA, USA*

Received 28 August 2002; revised 7 January 2005; accepted 7 January 2005

Abstract

While the predictive nature of the primate smooth pursuit system has been evident through several behavioural and neurophysiological experiments, few models have attempted to explain these results comprehensively. The model we propose in this paper in line with previous models employing optimal control theory; however, we hypothesize two new issues: (1) the medial superior temporal (MST) area in the cerebral cortex implements a recurrent neural network (RNN) in order to predict the current or future target velocity, and (2) a forward model of the target motion is acquired by on-line learning. We use stimulation studies to demonstrate how our new model supports these hypotheses. © 2005 Elsevier Ltd. All rights reserved.

Keywords: Oculomotor control; Medial superior temporal (MST) area; Predictive visual tracking; On-line fast learning; Forward model; Recurrent neural network

1. Introduction

Due to their narrow foveal vision, which has a viewing angle of only a few degrees, primates have to move their eyes to acquire accurate information on small moving targets in the environment. Smooth pursuit eye movements (SPEMs) perform this function and can achieve remarkable performance. For example, humans can maintain a velocity gain, i.e. the ratio of eye velocity to target velocity, of one up to a target speed of about 20°/s, while monkeys have been reported to even exceed this value. The accuracy of smooth pursuit is not only confined to constant velocity targets but has also been observed in periodic motion such as sinusoidal signals with frequencies of less than about 1 Hz (Dallos & Jones, 1963; Stark, Vossius, & Young, 1962; Westheimer, 1954).

Even a phase lead of the eyes can sometimes be observed in such experiments. Due to the information processing delays (e.g. 80–130 ms for human brain) in the visual pathways, the experimentally observed high performance of the smooth pursuit system cannot be achieved solely with standard negative feedback methods based on visual error signals. Under such delayed information processing, simple feedback control has a significant phase shift to the target signal, and thus some form of predictive control must take place (Pavel, 1990).

Several experimental results have been reported that also shed some light on the predictive nature of the smooth pursuit system. Morris & Lisberger (1983, 1987) demonstrated that monkeys were able to execute smooth pursuit with zero retinal slip by using a special target presentation technique called ‘target stabilization’. It is also known that monkeys can maintain smooth pursuit during blink periods, i.e. a sudden disappearance of the target for a brief moment (Churchland & Lisberger, 2000; Kawano, Shidara, Watanabe, & Yamane, 1994; Newsome, Wurtz, & Komatsu, 1988; Pola & Wyatt, 1997; Sakata, Shibutani, & Kawano, 1983). Such predictive compensation has been observed both in constant velocity and sinusoidally moving

* Corresponding author. Address: Graduate School of Information Science, Nara Institute of Science and Technology, 8916-5 Takayama-cho, Nara 630-0192, Japan. Tel.: +81 743 72 5981; fax: +81 743 72 5989.
E-mail address: tom@is.naist.jp (T. Shibata).

targets (Becker & Fuchs, 1985; Fukushima, Yamanobe, Shinmei, Fukushima, 2002; Whittaker & Eaholtz, 1982).

Therefore, it seems clear that SPEMs are a key to uncovering mechanisms for predicting the external world in the primate brain. In place of previous models, this article develops a SPEM model that employs a compact representation of the target motion that can be quickly learned in an on-line fashion based on visual error signals. By taking neuroanatomical findings into account, our model further suggests that the medial superior temporal (MST) area has the possibility of predicting target velocity using only signals that originate from visual information, without relying on efference copies of the oculomotor command or proprioceptive feedback.

2. Model development

2.1. Previous models

Pioneering computational models for SPEMs (Robinson, Gordon, & Gordon, 1986; Yasui & Young, 1975) attempted to cancel out the feedback signal in order to enable high velocity gain; their model works as a feedforward controller. Fig. 1 describes the essence of Robinson's model. In this model, the feedback signal with a delay Δ_1 is precisely canceled out by a positive feedback loop with the delay $\Delta_1 + \Delta_3$. However, their feedforward pathway still contains a significant delay determined by Δ_2 and τ such that this model cannot achieve zero-lag tracking of a sinusoidal signal. For instance, for a 1 Hz sinusoidal motion, the eye movement lags the target by more than 200 ms. Krauzlis and Lisberger proposed a model that employed nonlinear filters for velocity and acceleration of the retinal slip in their visual processing pathways (Krauzlis & Lisberger, 1994). Their model can reconstruct the SPEMs in their initiation phase as effectively as Robinson's model, but it cannot achieve zero-lag tracking of a sinusoidal signal similar to the Robinson's model, because it is essentially a feedback control model.

From the control-theoretic point of view, it is essential to have an internal representation of target motion that enables prediction of the current or future target velocity based on the past target state, e.g. position and velocity in the world coordinates. Bahill and McDonald (1983) proposed a theoretically sound control model based on predictive

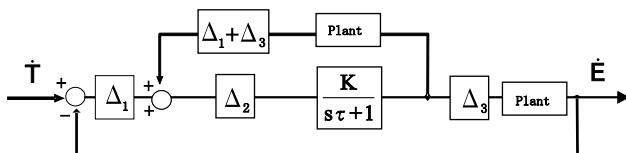


Fig. 1. A modified Robinson's model (Robinson et al., 1986) describing the essential property of the control system. \dot{T} is target velocity and \dot{E} is eye velocity. Δ_1 , Δ_2 and Δ_3 are delay times. Here, s denotes a Laplace transformation operator. τ is a time constant. K is a gain.

control. Their model reconstructed eye movement similar to that of humans where a sinusoidal or parabolic signal was presented periodically, but it required a priori knowledge of the target motion model. In contrast, our model below will acquire such a model by learning taking known biological constraints into account.

Another mechanism is a memory-based model that relies on the periodicity of the target by estimating the period, memorizing the entire retinal error over one period, and using the memorized retinal error to generate the appropriate oculomotor command (Banes & Grealy, 1992; Barnes & Wells, 1999). However, such a memory-based approach seems more artificial and less biologically plausible than the predictive control approach because (1) it requires a periodicity estimator that needs a specialized computation, and (2) at least in humans improvement in SPEM performance occurs continuously; if such an improvement is heavily dependent on the target periodicity, the improvement must be periodic. Thus, our work focuses on a predictive control model.

2.2. Neuroanatomy

From a neurophysiological point of view, the middle temporal (MT) area and medial superior temporal (MST) area seem to be intimately involved in smooth pursuit. Moreover, neurophysiological results support the idea that the major computation for the smooth pursuit maintenance phase is performed in area MST (Dürsteler, Wurtz, & Newsome, 1987; Kawano, Shidara, Watanabe, & Yamane, 1994). Kawano, Shidara, Watanabe, and Yamane. (1984) shed some light on the information processing taking place in the MST area. Roughly in the area that is now called MST, they found a group of neurons that responded to gaze velocity, i.e. the velocity of the gaze in the world coordinates. This result was supported by experiments in which the activities of the same neurons were very similar in either pure eye tracking of a sinusoid or vestibulo-ocular reflex (VOR) cancellation, where a target was moving sinusoidally and the head of the monkey was also externally moved sinusoidally, requiring the monkey to keep its eyes still and cancel the VOR in order to keep its gaze on the target. On the other hand, the same neurons had no discharge properties when the monkey was oscillated sinusoidally in the dark (a pure VOR task). Therefore, activity in these visual tracking neurons seems to originate from highly preprocessed visual inputs and not from efferent or afferent signals (related to eye movement). This point is crucial from the computational neuroscience point of view because it suggests that the major computation for smooth pursuit could be achieved in the desired trajectory space within the MST areas, and not in the motor command space.

Cortical eye fields are also thought to be involved in smooth pursuit (Tian & Lynch, 1996); in particular, the frontal eye field (FEF) has been intensively studied for smooth pursuit (Fukushima, Yamanobe, Shinmei,

Fukushima, Kurkin, & Peterson, 2002; Gottlieb, MacAvoy, & Bruce, 1994; MacAvoy, Gottlieb, & Bruce, 1991). This paper, however, is not concerned with the FEF due to the fact that the MST areas and the FEF have reciprocal connections, and their properties appear similar (Fukushima, Yamanobe, Shinmei, Fukushima, Kurkin et al., 2002; Newsome et al., 1988). At present, we do not have further information, such as the simultaneously recorded physiological data of the MST and the FEF, that would demand a modification of our model.

2.3. Our model

Fig. 2 depicts our conceptual control model of smooth pursuit mapped onto neuroanatomically plausible pathways. Without loss of generality, we treat only one rotational degree to highlight the principles of our control system—multiple degrees would require an appropriate replication of the circuit. In Fig. 2, the retinal slip \dot{E} is generated from the difference between the eye velocity \dot{E} and the target velocity \dot{x} , i.e.

$$\dot{e} = \dot{x} - \dot{E}. \quad (1)$$

Information on visual motion is processed hierarchically in the visual cortices, and finally reaches MT and MST for further analysis. From here, it is conveyed to the brain stem via DLPN and the cerebellum, thus allowing smooth pursuit to be maintained.

The physiological network in Fig. 2 itself is not novel; however, by assigning computations to its structure, a new view of smooth pursuit maintenance can be derived. This circuit consists of two subsystems: (i) a recurrent neural network (RNN) mapped onto MST, which receives the retinal slip with delays and predicts the current target motion, and (ii) an inverse dynamics controller (IDC) of the oculomotor system, mapped onto the cerebellum and the brainstem.

The first subsystem is the key point of our model. It receives retinal signals that convey the past target motion and eye motion and predicts the current target velocity. It is

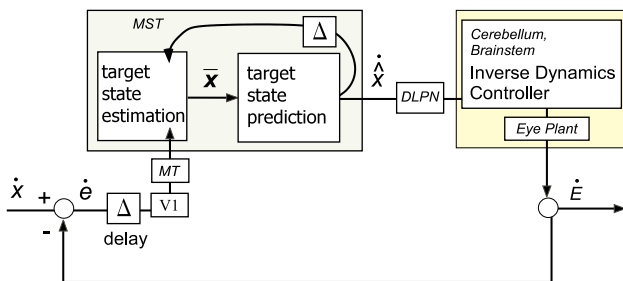


Fig. 2. Conceptual control model mapped onto physiologically plausible pathways. We assume that the recurrent network (RNN) exists in the higher visual cortex areas and that the cerebellum and brainstem together form the inverse dynamics controller (IDC) of the eye. The delay element Δ represents the total delay in the visual pathway. See text for other abbreviations.

theoretically possible that one predicts the future target velocity by observing the target state \mathbf{x} at a time with the knowledge of the forward model of the target motion. Because the brain cannot observe the target state directly, it needs to estimate the state based on Δ -time delayed retinal slip information. Eq. (2) represents the prediction of the current target velocity $\dot{\hat{x}}(t)$ from an estimated past target state $\bar{\mathbf{x}}(t - \Delta)$ by the function f :

$$\dot{\hat{x}}(t) = f(\bar{\mathbf{x}}(t - \Delta)), \quad (2)$$

where f essentially corresponds to the Δ -time discretized target dynamics. Applying f recurrently computes a predicted future target state. Note that the information in the state variables in $\bar{\mathbf{x}}(t - \Delta)$ should suffice for calculating $\dot{\hat{x}}(t)$.

Based on theory and experiment showing that the cerebellum and brainstem together act as an inverse dynamics controller of the oculomotor plant (Kawato, 1999; Shidara, Kawano, Gomi, & Kawato, 1993), we assume that the IDC has the capability to cancel the dynamics of the eye plant, and, for the moment, that this is done perfectly, making it valid to write

$$\dot{E}(t) = \dot{\hat{x}}(t). \quad (3)$$

Under this assumption, neither the IDC nor the eye plant needs to be detailed in Fig. 2.

The state estimator $\bar{\mathbf{x}}(t - \Delta)$ in Eq. (2) results from

$$\bar{\mathbf{x}}(t - \Delta) = \hat{\mathbf{x}}(t - \Delta) + \mathbf{K}(\mathbf{x}(t - \Delta) - \hat{\mathbf{x}}(t - \Delta)). \quad (4)$$

The first term of the right-hand side of this equation is the predicted state at time $(t - \Delta)$, while the second term is the prediction error multiplied by a weight matrix \mathbf{K} , which corrects the predicted state by means of the $(t - \Delta)$ delayed sensory signal. Essentially, Eq. (4) is a part of the update equations of a Kalman filter (see Discussion 4.4). Since we assume $\mathbf{K} = \mathbf{1}$ throughout this paper, the essence of Eq. (4) can be reduced to $\bar{\mathbf{x}}(t - \Delta) = \mathbf{x}(t - \Delta)$, i.e. the simplest form of an estimator. Given that $\mathbf{x}(t - \Delta)$ is not directly observable, Eq. (4) is nevertheless needed to compute $\mathbf{x}(t - \Delta)$ by noting the following transformations based on the assumption in Eq. (3) and the retinal slip definition in (1):

$$\begin{aligned} \dot{\hat{x}}(t - \Delta) &= \dot{\hat{x}}(t - \Delta) + k(\dot{x}(t - \Delta) - \dot{\hat{x}}(t - \Delta)) \\ &= \dot{\hat{x}}(t - \Delta) + k(\dot{x}(t - \Delta) - \dot{E}(t - \Delta)) \\ &= \dot{\hat{x}}(t - \Delta) + k\dot{e}(t - \Delta) \\ &= \dot{\hat{x}}(t - \Delta) + \dot{e}(t - \Delta). \end{aligned} \quad (5)$$

The last equation assumes $k = 1$. $\bar{\mathbf{x}}(t - \Delta)$ is obtained by integrating $\dot{\hat{x}}(t - \Delta)$ (See Section 4.1 for a discussion on biological plausibility of the positional signals). Thus, state estimation can operate correctly based on the internal feedback of $\dot{\hat{x}}(t)$ and the delayed retinal slip signal $\dot{e}(t - \Delta)$.

The final issue for our model is how to acquire the target dynamics. It has been found that the gain and phase of biological smooth pursuit can be gradually improved by presenting the target motion repetitively (Dallos & Jones, 1963). We regard such gradual improvement as evidence for on-line learning of the target dynamics, which can be formulated as follows.

At time t , the predictor can only see the delayed estimated target state $\bar{\mathbf{x}}(t - \Delta)$. By making the parameter vector \mathbf{w} in the target state predictor f explicit, the target velocity prediction is

$$\dot{\hat{x}}(t) = f(\bar{\mathbf{x}}(t - \Delta), \mathbf{w}(t)) \equiv f(t), \quad (6)$$

where \mathbf{w} needs to be adjusted by the learning system. Note that the predictor predicts only the target velocity instead of the complete target state in accordance with biological constraints, i.e. that only velocity information is conveyed in the visual pathway, and the command generated in each oculomotor behavior pathway is equally interpreted as a velocity command. Let the loss function J be the simple squared prediction error

$$J(t) = \frac{1}{2} \dot{e}(t)^2 = \frac{1}{2} (\dot{\hat{x}}(t) - \dot{E}(t))^2. \quad (7)$$

Employing Eqs. (3) and (6), a gradient descent learning rule for \mathbf{w} can be written as

$$\frac{dw_i(t)}{dt} = -\varepsilon \frac{\partial J(t)}{\partial w_i} = \varepsilon \frac{\partial f(t)}{\partial w_i} \dot{e}(t), \quad (8)$$

with ε denoting the learning rate.

3. Simulation results

3.1. Simulation setup

In order to verify that our model can achieve smooth pursuit with gain one and zero-latency, we conducted two evaluations by simulation. In one setup, the input was a ramp input with a constant velocity of 0.5 rad/s, and in the other setup, a sinusoidal input was chosen with a frequency of 1.0 Hz. Note that the dynamics of these inputs is a second-order linear system, which guarantees that the current target velocity can be predicted by the past target state, i.e. position and velocity.

Fig. 3 is the actual model used for simulations in control-theoretic detail. Since the eye plant of primates can be approximated by a second-order linear dynamical system (Keller, 1973), a linear inverse dynamics model suffices for feedforward control of the eye system. It receives as input the desired eye angular position, velocity, and acceleration. The dark shaded block in Fig. 3 corresponds to the RNN. According to Yamamoto, Kobuyashi, Takemura, Kawano, and Kawato (2000), the eye velocity and acceleration commands are generated by Purkinje cells, but the eye position command is generated elsewhere, possibly in

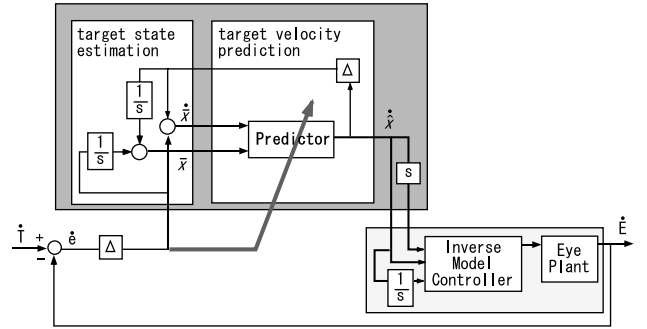


Fig. 3. Second-order linear model. The dark shaded block corresponds to the RNN in Fig. 2. Here, s denotes a Laplace transformation operator. In this diagram, s stands for differentiation and $1/s$ for integration.

the brainstem. We also know that the activities of Purkinje cells in smooth pursuit originate in the activities of the MST area. Thus, while the predicted target velocity and acceleration are calculated in the RNN, the predicted target position is not.

To enable the RNN to learn the target dynamics of constant velocity and sinusoidal motion, a second-order linear system suffices to represent their dynamics. Theoretically, when the target has second-order linear dynamics, $\mathbf{x}(t) = A\mathbf{x}(t - \Delta)$, with the target position x , velocity \dot{x} , the state vector $\mathbf{x} = [x \ \dot{x}]^T$, and Δ -time discretized state transition matrix A . To predict the target velocity, only the second row of A is required, denoted as \mathbf{w} :

$$\dot{\hat{x}}(t) = \mathbf{w}^T \bar{\mathbf{x}}(t - \Delta). \quad (9)$$

It is important that the causality between \hat{x} and \dot{E} be maintained so that Eq. (8) effectively decreases the error function J . Because the predictor cannot see $\dot{e}(t)$; at time t , we use Eq. (10), where in the right-hand-side, time is shifted by Δ -time to the past.

$$\frac{dw_i(t)}{dt} = \varepsilon \frac{\partial f(t - \Delta)}{\partial w_i} \dot{e}(t - \Delta) \quad (10)$$

In each simulation, we employed the recursive least squares algorithm (RLS) (Ljung & Soderstrom, 1986) for learning because its fast and guaranteed convergence mimics the quick and high-gain learning of humans. See Appendix for our use of RLS in detail.

Using MATLAB/SIMULINK, the simulation model was built as a continuous system. Only the predictor, a recurrent network, was run with discrete update times, ranging between 30 and 200 Hz to test the robustness of the system. The delay in the visual pathway was set to values between 50 and 150 ms, corresponding to the spectrum of values reported in the neurobiological literature. Within these ranges, our model worked well in all simulations, although it was necessary to tune the forgetting factor in RLS as a function of the predictor's update frequency.

All of our learning experiments started from scratch, i.e. with all initial states including the weights of the learning system set to zero. Note that the learned result does not

depend on the initial states because our model is linear. However, we chose zero because large initial values cause the system to become temporarily unstable.

According to Keller (Keller, 1973), the eye plant was modeled as a second-order linear system (Eq. (11)) with inertia term M , viscous term B , and spring term K set to 0.02, 0.08, and 4.14, respectively. The term u is the input torque:

$$M\ddot{x} + B\dot{x} + Kx = u. \quad (11)$$

3.2. Results

Fig. 4 shows that smooth pursuit was successfully accomplished in the case of the ramp input. Fig. 4(B) presents the time course of the eye velocity rapidly approaching the target velocity, and (C) depicts the time course of the retinal slip, quickly reaching zero. Fig. 4(B) illustrates a ringing in the eye velocity, which is mainly caused by the parameter set to enable fast learning. It is known that the eye velocity during tracking of the ramp motion typically exhibits such ringing, whose frequency is about 3–5 Hz. However, our simulation gives only around 2-Hz ringing and does not help to explain the biological data. This is thought to be the limitation of a linear system, and will be improved by introducing nonlinearity as discussed in Robinson et al. (1986). In the case of

a 100-ms delay, the discrete state transition matrix of a ramp input is expected to be

$$\mathbf{A} = \begin{pmatrix} 1 & 0.1 \\ 0 & 1 \end{pmatrix};$$

the converged weights around 0.02 and 0.98 in Fig. 4(D) were very close to these optimal values, i.e. 0 and 1 from the second row of \mathbf{A} .

The results of the second experiment with sinusoidal target motion at 1.0 Hz and an amplitude of 0.5 rad are illustrated in Fig. 5. Again, smooth pursuit learning was successful in neatly converging regression coefficients. Theory predicts an optimal weight vector of $[-3.6931 \ 0.8090]^T$. The actual acquired final weight vector is $[-3.678 \ 0.7899]^T$, which is close to our expectations.

These results were acquired with one set of hyperparameters in RLS that we had finely tuned. However, one could still claim that learning speed is much slower than in human, and that the transient response at the stimulus onset is crude. While our model is not designed to explain the initiation phase of smooth pursuit, an appropriate prior in RLS, such as constant velocity motion, can improve the initial and transient response. Fig. 6 demonstrates the effect of the prior. In this case, the target motion was generated by the same sinusoidal signal used in Section 3, but the initial weights for the estimated target position and velocity were

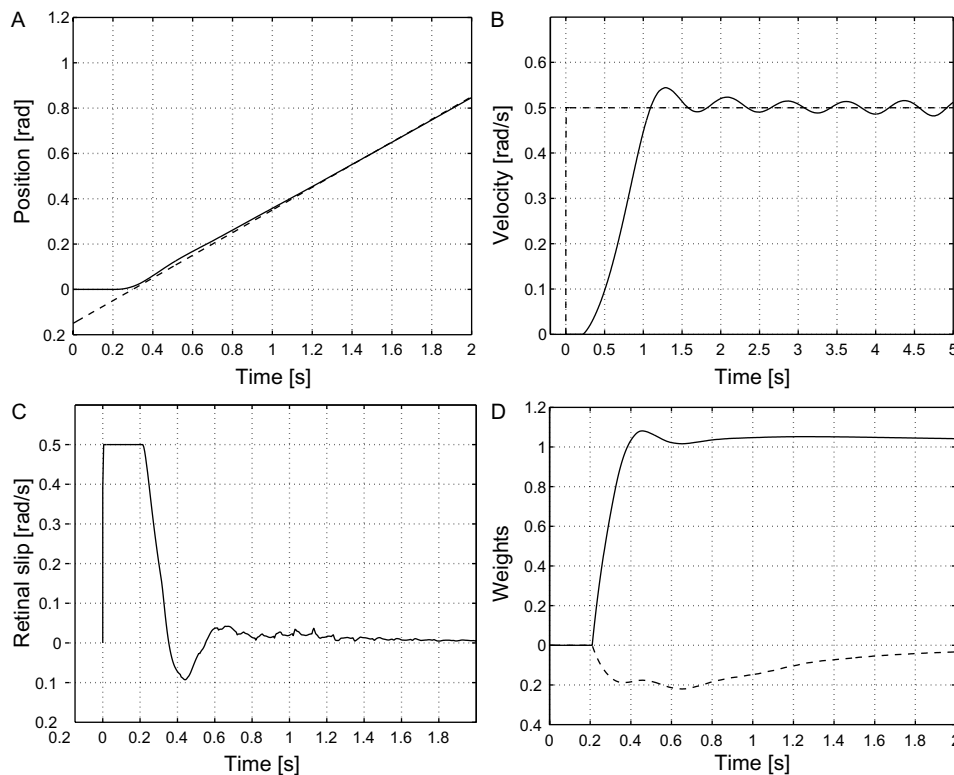


Fig. 4. Simulation results in the case of a constant velocity motion of the target. (A) Time course of the angular position of the visual target (dotted) and the eye (solid). (B) Time course of the velocity of the visual target (dotted) and the eye (solid). (C) Time course of the retinal slip. (D) Time course of the weight for the position input (dotted) and the velocity input (solid) of the learning system.

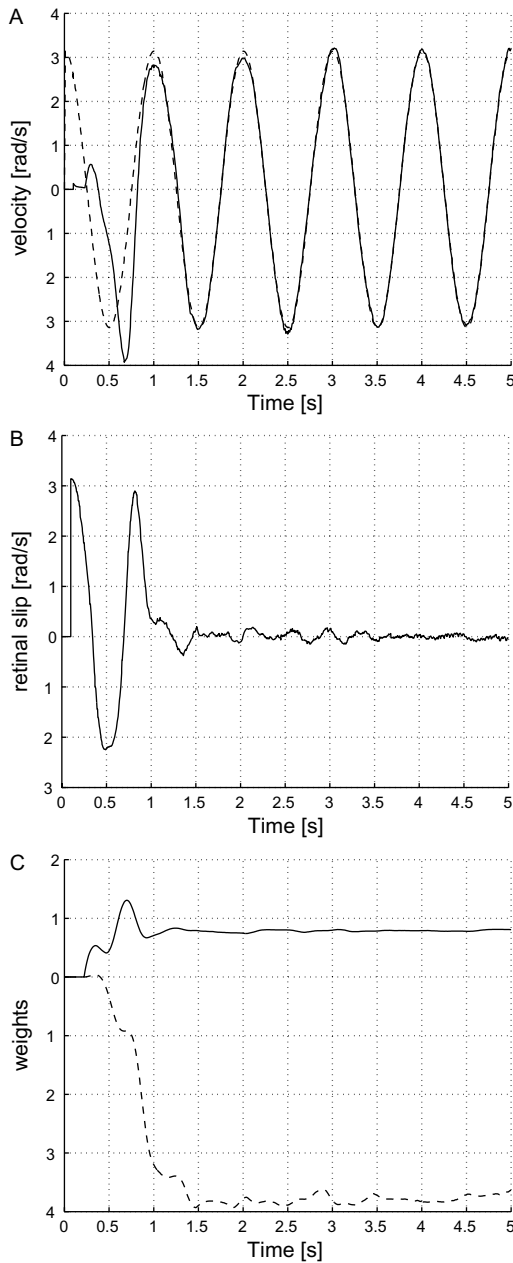


Fig. 5. Simulation results in case of a sinusoidal motion of the target. (A) Time course of the velocity of the visual target (dotted) and the eye (solid). (B) Time course of the retinal slip. (C) Time course of the weight for the position input (dotted) and the velocity input (solid).

varied. Fig. 6 shows that the initial response of weights set to $[0\ 0]^T$ is very poor, while the other two types of weight initialization provided a vivid initial response.

Fig. 7 demonstrates that our model can continue generating proper eye velocity during blink periods, as described in Section 2.3. In particular, Fig. 7(B) illustrates the eye acceleration changes during the blink periods by means of the appropriate prediction based on the knowledge of target dynamics. For these simulations, the knowledge of the target dynamics was given from the beginning.

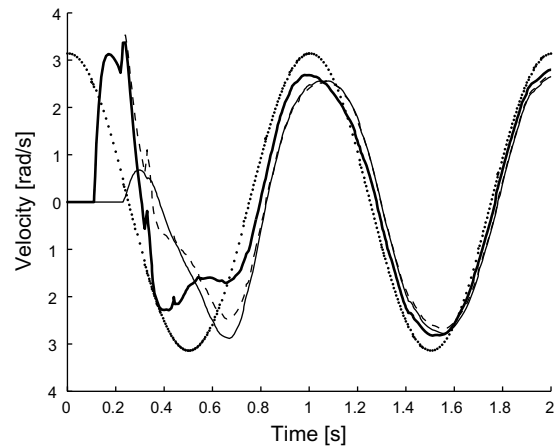


Fig. 6. Learning of the forward model of a sinusoidal signal with prior knowledge of the target motion. The dotted line shows the target motion. The solid line was generated by our model with the initial weight vector $[0\ 0]^T$. The dashed line resulted from our model with the initial weight vector $[0\ 1]^T$, which means a constant velocity motion was assumed. The thick solid line corresponds to the case where the initial weight vector was $[-2\ 1]^T$, which is closer to the theoretically correct values.

While we have assumed that the inverse dynamics controller (IDC) consisting of the cerebellum and the brain stem is perfect, it is useful to consider what the recurrent neural network (RNN) in MST would do in the case where the perfect IDC assumption does not apply. For this purpose, the key idea is to imagine that an imperfect IDC and the eye plant together form a new plant (extended plant). In this case, the RNN has to learn a composite function that includes the target dynamics and the dynamics of the extended plant in order to minimize the retinal slip. Given that the extended plant in our example is at most second-order linear, the second-order linear system of the RNN should be able to compensate for IDC inaccuracies perfectly. Figs. 8 and 9 present simulation results supporting our expectation. In the case of Fig. 9(A), with respect to the actual target velocity, the amplitude of the predicted target velocity is slightly greater and its phase is delayed, which is theoretically necessary to compensate for the imperfect IDC, where the spring constant is reduced by 50%. In the case of Fig. 9(B), since the viscous term of the IDC is 50% of the true value, the theoretically required advanced phase and increased amplitude can be observed correctly in our simulation. Fig. 9(C), to compensate for two imperfect parameters in the IDC, the amplitude of the predicted target velocity significantly increases, and its phase is almost the same as the actual target velocity. We also tested a case where the mass term was changed and observed no problem in successful learning. Note that the purpose of these experiments is to relax the former assumption of the perfect IDC. Removing the IDC causes SPEMs to be absent and learning to break down; the IDC is downstream from the predictor and is thus inherently necessary to move the eyes.

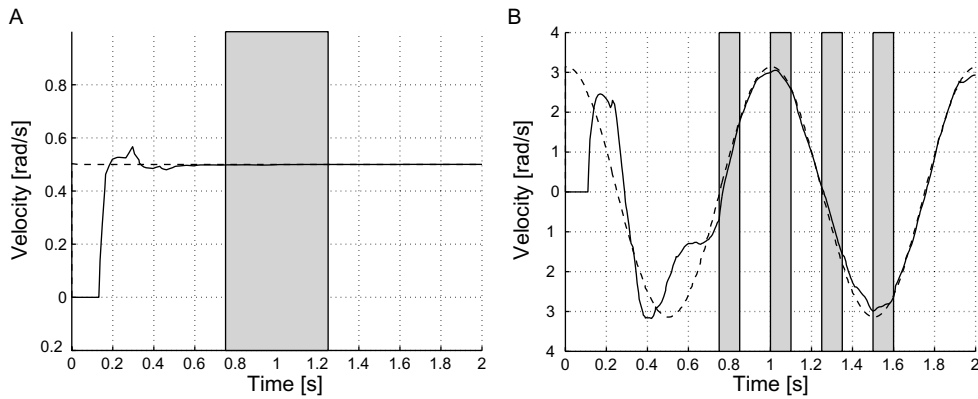


Fig. 7. Simulation results of blink experiments. Here, (A) and (B) show the time course of target velocity (dotted) and eye velocity (solid) when the input is a constant velocity motion and a sinusoidal signal, respectively. The dark shaded blocks represent blink periods. The blink period was set to 500 ms in (A) and 100 ms in (B).

4. Discussion

We have presented a computational model employing a predictive controller with fast learning of the target dynamics enables zero-lag SPEMs. In our model, the representation of the target motion is much simpler than the memory-based model, and learning proceeds quickly, decreasing the retinal slip without waiting for one period of the target motion. Our

model can also maintain SPEMs during the target blinking. We have also demonstrated that the learning predictor of target motion can be realized by the cortical recurrent neural network, assumed to exist in the MST area, even if there is no efference copy of the eye.

As our model primarily emphasized a control-theoretic development, the following sections focus on its neurophysiological plausibility.

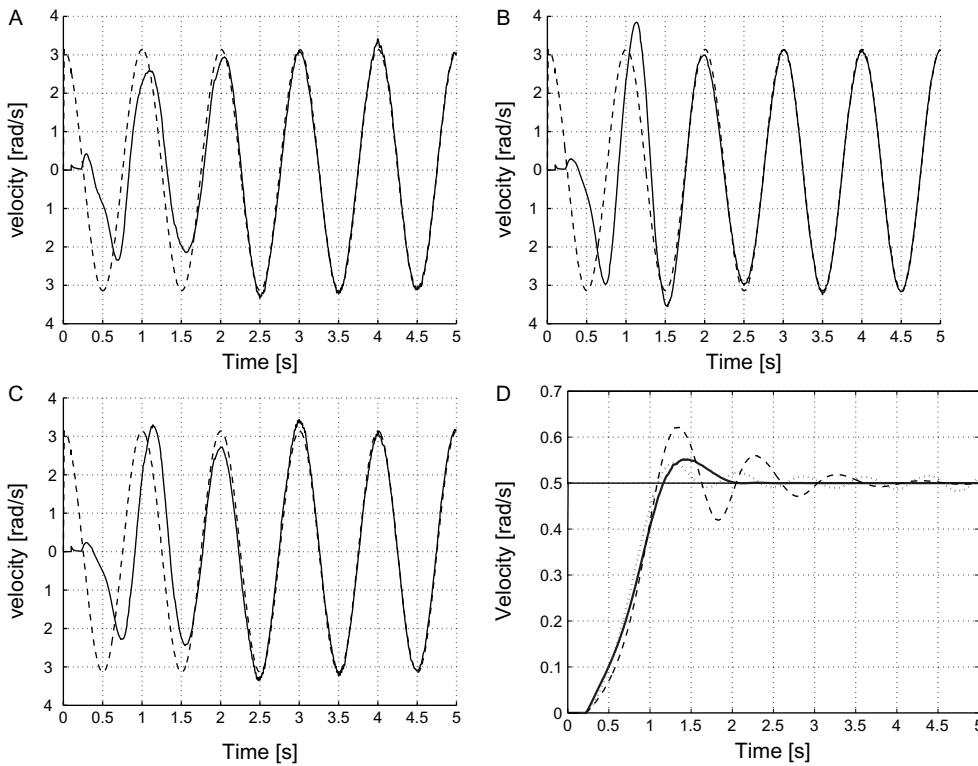


Fig. 8. Simulation results in the case of imperfect inverse dynamics controllers. (A–C) show the results when the input is a sinusoidal signal, while (D) presents the results when the input is a ramp. Time course of the angular velocity of the visual target (dotted) and the eye (solid). (A) The spring term is reduced by 50%. (B) The viscous term is reduced by 50%. (C) Both the spring term and the viscous term are reduced by 50%. (D) Solid line is the target velocity. Thick, dotted, and dashed lines are the generated eye velocities when the spring term, the viscous term, and both terms are reduced by 50%, respectively.

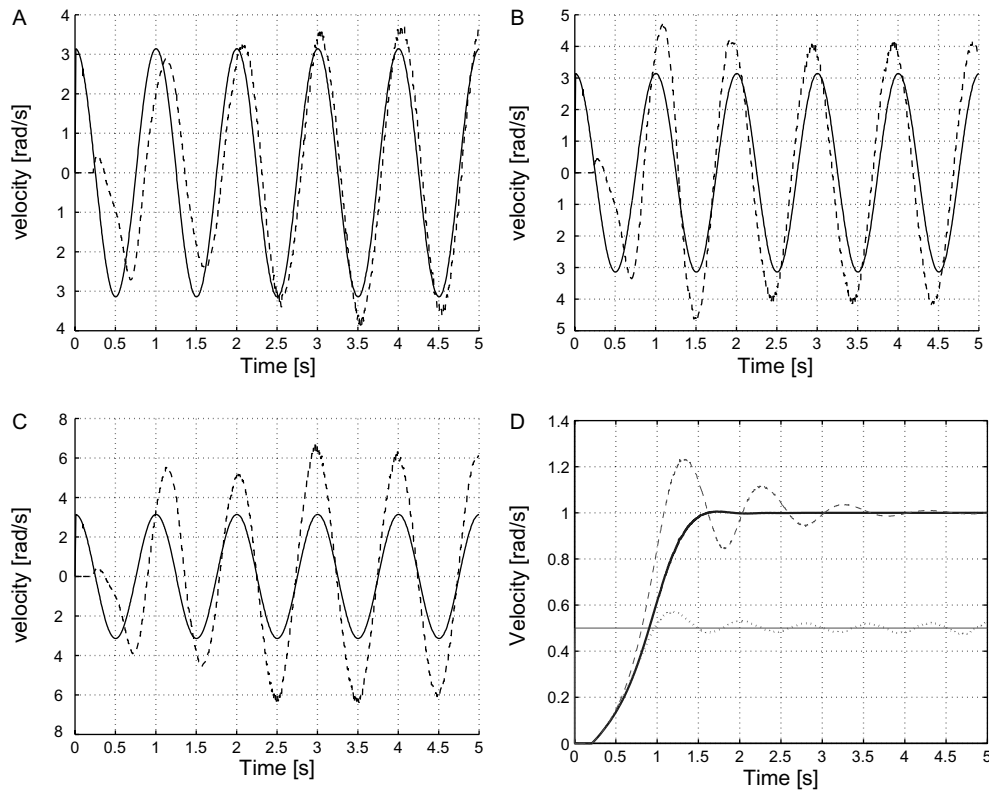


Fig. 9. Simulation results in the case of imperfect inverse dynamics controllers. (A–C) show the results when the input is a sinusoidal signal, while (D) presents the results when the input is a ramp. Time course of the angular velocity of the visual target (solid) and the predicted target (dashed). (A) The spring term is reduced by 50%. (B) The viscous term is reduced by 50%. (C) Both the spring term and the viscous term are reduced by 50%. (D) Solid line is the target velocity. Thick, dotted, and dashed lines are the predicted target velocities when the spring term, the viscous term, and both terms are reduced by 50%, respectively.

4.1. Use of estimated target position

In general, we assume the inverse model controller implemented in the cerebellum and brainstem is perfect, and that the forward model of the target motion is generated in the RNN of the MST area. While the target-state estimator in the RNN estimates both target position and velocity (Fig. 3), usually only velocity is referred to in neurophysiological studies of smooth pursuit maintenance in MST, e.g. (Komatsu & Wurtz, 1988a; Newsome et al., 1988). However, in the monkey MSTd area, Squatrito and Maioli (1997) found eye-position modulated neurons which were also activated during SPEMs as well as neurons activated but not influenced by eye position during SPEMs. DeSouza, Dukelow, and Villis (2002) found eye-position modulation of the brain activities in MT+ in their human fMRI study. According to these studies in which a target position and an eye position were not distinguishable during SPEMs, the use of a target position in our model is not implausible.

Alternatively, two other implementations can be considered. One is for estimating the target velocity and acceleration instead of the target position and velocity. This alteration would not harm our model since this

information still suffices to predict the current target velocity and would also be neurophysiologically plausible (Takemura, Inoue, Gomi, Kawato, & Kawano, 2001). The other possible method is to employ a tapped delay line (TDL) model, where target velocities at several delay periods are maintained and used to predict the current target velocity. As benefits of this method, only velocity signals are required, and it can theoretically represent higher-order linear motion by simply increasing the number of taps. Although there is so far no direct evidence whether such a TDL model is implemented in MST, Bi and Poo (1999) demonstrated the possibility of the existence of a TDL in the brain through their experiments with cultured hippocampal neurons. What they accounted for is that polysynaptic transmission pathways combined with spike-timing-based synaptic modifications provide a TDL.

If such a TDL is available in the MST area, an interesting issue is to what degree higher-order linear dynamics of the target motion can be learned in humans. Constant velocity or sinusoidal motion has been typically used for the stimulus, i.e. motion generated by either a first- or second-order linear system. However, we can provide a wide variety of other stimuli from the viewpoint of linear

systems. For instance, Bahill and McDonald (1983) used a periodic parabolic stimulus. They also reported that subjects were able to track a cubic wave form with zero-latency. In future work, we will conduct a systematic and comprehensive investigation of the abilities of the human smooth pursuit with more complicated target motion stimuli, and we will also monitor the course of learning.

4.2. Initial response

We have employed the recursive least squares algorithm (RLS) for learning, since it is fast and guarantees convergence. We hoped it would mimic the quick and high-gain learning of humans; however, as demonstrated in Fig. 5, the initial response was poor and the converging speed was slower than that in humans. Consequently, we have conducted research to determine if an appropriate prior in RLS could solve these problems. Fig. 6 shows that the prior can significantly improve performance, although we might claim that the converging speed is still slower than in humans. For instance, zero-latency tracking can occur after only one quarter of a target motion cycle (Bahill & McDonald, 1983) if the subjects are experienced with the target motion. To explain this fact, Bahill and McDonald proposed a ‘menu selection’ method, which enables human-like initial performance if the brain selects the correct target dynamics model from the ‘menu’. In our model, this corresponds to the case where the prior weights in RLS completely or mostly describe the target dynamics, obviously leading to a good initial response. In relation to this issue, it would be interesting to investigate such issues as how long we can maintain a model image, how learning another model affects the current memory, and how and where the model images are stored.

4.3. Learning and prediction

The learning rule in Eq. (10) is a form of Hebbian learning. The right side consists of the multiplication of a quantity correlated with the estimated target state, $\partial f(t-\Delta)/\partial w_i$, and the retinal slip, $\dot{e}(t-\Delta)$. These quantities are available in the MST area. The mechanism for keeping the information $\partial f(t)/\partial w_i$ for a Δ -time could be realized by a signal transduction in MST neurons. It has been investigated whether this type of temporal window in the synaptic plasticity is mediated by such a signal transduction in Purkinje cells (Houk, Singh, Fisher, & Barto, 1990; Kuroda, Schweifhofer, & Kawato, 2001; Wang, Denk, & Häusser, 2000). Moreover, spike-timing dependent plasticity (STDP) in hippocampal neurons has been reported for the temporal window (Bi & Poo, 1998). The STDP reported has a narrow temporal window that is most effective at around ± 20 ms for long-term potentiation (LTP) and long-term depression (LTD), and it reaches half its effectiveness at around ± 40 ms, leading to

little effect at around ± 100 ms. Although current knowledge of the STDP is insufficient for realizing the time-alignment of 80–130 ms assumed in this paper, this idea has potential because the temporal window of MST neurons has not been studied yet, and the window contains regional variabilities (Feldman, 2000; Song & Abbott, 2001).

4.4. Optimal estimation

To date, although we have no strong evidence that MST implements an optimal estimation algorithm such as RLS, some supportive studies have been conducted toward interpreting cortical processing in light of estimation theory. In neurophysiology, as has been found for other cortical areas such as M1 (Georgopoulos, Schwartz, & Kettner, 1986; Todorov, 2000), there is evidence for population coding in MT (Lisberger & Movshon, 1999) in addition to MST (Takemura, Inoue, Kawano, & Miles, 2001). Computational neuroscientists have been attempting to understand population coding from the viewpoint of optimal estimation (Pouget, Zhang, Deneve, & Latham, 1998; Rao, 1999; Rao & Ballard, 1999; Salinas & Abbott, 1995). Accompanied by behavioral evidence, it has also been hypothesized that internal models are represented in a probabilistic way by neural population codes in order to carry out optimal estimation for perception (Burgi & Yuille, 2000; Zemel, Dayan, & Pouget, 1998) and control (Witney, Goodbody, & Wolpert, 2000).

Note that the model we propose already has a structure similar to a Kalman filter, which is the most famous on-line linear probabilistic minimum variance estimator. Like the Kalman filter, the RNN consists of two steps: target-state estimation and target-state prediction. Furthermore, the Kalman filter maintains the confidence of estimation and uses the Kalman gain \mathbf{K} in the target state estimation step. Eq. (4) already includes this style of computation, so only the derivation of \mathbf{K} would need to be changed to conform to the on-line Kalman filter equations.

A true Kalman filter implementation would give us the additional benefit of improving our smooth pursuit model as follows. In this paper, we derived a smooth pursuit model based on behavioral and physiological experimental results. However, our present model cannot reproduce one experimental finding, i.e. the smooth pursuit blink. Our current model keeps predicting the target state forever without retinal slip information after learning is completed, as shown in Fig. 7. To reproduce the gradual reduction in the eye velocity during the smooth pursuit blink that was observed in biological data, two mechanisms could be considered, based on the common assumption that somehow the confidence of the target state is accessible. Since there is no visual information available during blink, the first idea is that a part of the brain monitoring the prediction confidence directly suppresses the MST area (Taguchi, Tabata, Shibata,

Doya, & Kawato, 2002). For example, either the frontal pursuit area pointed out by Tanaka et al. (Taguchi, Tabata, Shibata, & Kawato, 2004; Tanaka & Lisberger, 2001), or the frontal eye field can be candidate areas for this task. Alternatively, we could imagine that such behavior during smooth pursuit blink could be accomplished by population dynamics in the MST area and the conversion of its output by the cerebellum (Yamamoto, Kobayashi, Takemura, Kawano, & Kawato, 2002).

4.5. Role of subregions in MST

Cells in the MST area can mainly be divided into a dorsal medial (MSTd) and a lateral ventral (MSTl) region (Komatsu & Wurtz, 1988a; Tanaka, Sugita, Moriya, & Saito, 1993). The MSTd cells respond best to a large moving pattern rather than to small spots of light, while cells in MSTl respond better to the small spots. Further differential functional characteristics of cells in these two areas have been reported.

The MSTl neurons play significant roles in smooth pursuit in both its initiation and maintenance phases through lesions (Dürsteler & Wurtz, 1988) or electrical stimulation studies (Komatsu & Wurtz, 1989). Their activities rapidly attenuate during blink periods. Self-induced motion drives their activities preceding the onset of SPEM (Erickson & Their, 1991). The responses of neurons in the MSTl changed when a stimulus in the region surrounding the excitatory center of the receptive field was added to a stimulus falling in the center of the field, which could facilitate the perceptual segmentation of a moving object from its background (Eifuku & Wurtz, 1998).

On the other hand, while the MSTd neurons maintain their activities during blink periods (Newsome et al., 1988), lesion or electrical stimulation of MSTd would have little effect on pursuit eye movement (Dürsteler & Wurtz, 1988; Komatsu & Wurtz, 1989). The role of MSTd neurons for smooth pursuit could at least be to suppress the optokinetic nystagmus (OKN) response (Komatsu & Wurtz, 1988b).

We could relate the above knowledge to our model to some extent: lesion or electrical stimulation studies have shown cells in MSTl are crucial for smooth pursuit. They seem suitable for tracking a small target due to their preference for the target size as well as their capability of perceptual segmentation. Furthermore, the MSTl neurons can be predictive. Thus, the RNN part of our model might be achieved by the MSTl neurons.

We could also incorporate MSTd into our model. Based on lesion or electrical stimulation studies for MSTd, cells in MSTd seem to be not essential for smooth pursuit. However, this property could correspond to the target state estimator in our model. Namely, these disturbances may have been filtered out by the MSTd neurons. These neurons have a large receptive field, and they may integrate many MT and MSTl neurons as well as MSTd neurons, which are suitable for estimating the target state.

Appendix A. Fast learning by recursive least squares (RLS)

Originally, RLS was formulated as in Eqs. (A1) and (A2), where \mathbf{w} is the vector of regression parameters to be estimated, \mathbf{P} is the inverted covariance matrix of the input data, \mathbf{x} is the input vector, y is the output, and \hat{y} is the predicted output. A forgetting factor λ is discussed below.

$$\mathbf{P}(t) = \frac{1}{\lambda} \left[\mathbf{P}(t - \Delta) - \frac{\mathbf{P}(t - \Delta)\mathbf{x}(t)\mathbf{x}(t)^T\mathbf{P}(t - \Delta)}{\lambda + \mathbf{x}(t)^T\mathbf{P}(t - \Delta)\mathbf{x}(t)} \right], \quad (\text{A1})$$

$$\mathbf{w}(t) = \mathbf{w}(t - \Delta) + \frac{\mathbf{P}(t)\mathbf{x}(t)}{\lambda + \mathbf{x}(t)^T\mathbf{P}(t)\mathbf{x}(t)} (y(t) - \hat{y}(t)), \quad (\text{A2})$$

$$\hat{y}(t) = \mathbf{w}(t)^T \mathbf{x}(t). \quad (\text{A3})$$

Eq. (A2) shows that normal RLS requires the presence of a target output y in the update rules. As described in the introduction, the predictor cannot see this target output directly, but it can utilize the retinal signals as the prediction error. Thus, for our smooth pursuit, Eq. (A2) needs to be modified to:

$$\mathbf{w}(t) = \mathbf{w}(t - \Delta) + \frac{\mathbf{P}(t)\mathbf{x}(t)}{\lambda + \mathbf{x}(t)^T\mathbf{P}(t)\mathbf{x}(t)} \dot{e}(t + 1). \quad (\text{A4})$$

This strategy corresponds to training RLS on ‘fake’ targets, i.e. $y = \hat{y}(t) + \dot{e}$. Initially, these fake targets are fairly distant from the true targets, such that RLS is actually trained on incorrect data. For this purpose, one needs to forget data from early training, accomplished by the forgetting factor λ , which lies in the $[0, 1]$ interval. For $\lambda = 1$, no forgetting takes place, while for smaller values, older values in the matrix \mathbf{P} are exponentially forgotten. Essentially, the forgetting factor ensures that the prediction of RLS is only based on $1/(1 - \lambda)$ data points. This forgetting strategy also enables the predictor to be adaptive to the changes in the target dynamics.

Another important element of Eq. (A4) is that it explicitly shows the requirement for the time alignment of the predictor output and the error since the learning module cannot see $\dot{e}(t + 1)$ at time t . Thus, all variables in Eq. (A4) need to be delayed by one time step, which requires the storage of some variables for a short time in memory.

References

- Bahill, A., & McDonald, J. (1983). Model emulates human smooth pursuit system producing zero-latency target tracking. *Biological Cybernetics*, 48, 213–222.
- Barnes, G., & Grealy, M. (1992). Predictive mechanisms of head-eye coordination and vestibulo-ocular reflex suppression in humans. *Journal of Vestibular Research*, 2, 193–212.
- Barnes, G., & Wells, S. (1999). Modelling prediction in ocular pursuit. In W. Becker, H. Deubel, & T. Mergner (Eds.), *Current oculomotor research* (pp. 97–107). Plenum Press: New York.

- Becker, W., & Fuchs, A. (1985). Prediction in the oculomotor system: smooth pursuit. *Experimental Brain Research*, 57, 562–575.
- Bi, G., & Poo, M. (1998). Synaptic modifications in cultured hippocampal neurons: Dependence on spike timing, synaptic strength, and postsynaptic cell type. *Journal of Neuroscience*, 18(24), 10464–10472.
- Bi, G., & Poo, M. (1999). Distributed synaptic modification in neural networks induced by patterned stimulation. *Nature*, 401, 792–796.
- Burgi, P., & Yuille, A. (2000). Probabilistic motion estimation based on temporal coherence. *Neural Computation*, 12, 1839–1867.
- Churchland, M., & Lisberger, S. (2000). Apparent motion produce multiple deficits in visually guided smooth pursuit eye movements of monkeys. *Journal of Neurophysiology*, 84(1), 216–235.
- Dallos, P., & Jones, R. (1963). Learning behaviour of the eye fixation control system. *IEEE Transactions on Automatic Control*, AC-8, 218–227.
- DeSouza, J., Dukelow, S., & Vilis, T. (2002). Eye position signals modulate early dorsal and ventral visual areas. *Cerebral Cortex*, 12, 991–997.
- Dürsteler, M., & Wurtz, R. (1988). Pursuit and optokinetic deficits following chemical lesions of cortical areas MT and MST. *Journal of Neurophysiology*, 60(3), 940–965.
- Dürsteler, M., Wurtz, R., & Newsome, W. (1987). Directional pursuit deficits following lesions of the foveal representation within the superior temporal sulcus of the macaque monkey. *Journal of Neurophysiology*, 57(5), 1262–1287.
- Eifuku, S., & Wurtz, R. (1998). Response to motion in extrastriate area MSTl: Centresurround interactions. *Journal of Neurophysiology*, 80(1), 282–296.
- Erickson, R., & Their, P. (1991). A neuronal correlate of spatial stability during periods of self-induced visual motion. *Experimental Brain Research*, 86(3), 608–616.
- Feldman, D. (2000). Timing-based LTP and LTD at vertical inputs to layer II/III pyramidal cells in rat barrel cortex. *Neuron*, 27, 45–56.
- Fukushima, K., Yamanobe, T., Shinmei, Y., & Fukushima, J. (2002). Predictive responses of periaruate pursuit neurons to visual target motion. *Experimental Brain Research*, 145, 104–120.
- Fukushima, K., Yamanobe, T., Shinmei, Y., Fukushima, J., Kurkin, S., & Peterson, B. (2002). Coding of smooth eye movements in three-dimensional space by frontal cortex. *Nature*, 419, 157–162.
- Georgopoulos, A., Schwartz, A., & Kettner, R. (1986). Neuronal population coding of movement direction. *Science*, 233, 1416–1419.
- Gottlieb, J., Macavoy, M., & Bruce, C. (1994). Neural responses related to smooth-pursuit eye movements and their correspondence with electrically elicited smooth eye movements in the primate frontal eye field. *Journal of Neurophysiology*, 72(4), 1634–1653.
- Houk, J., Singh, S., Fisher, C., & Barto, A. (1990). *Neural networks for control, chapter 13 an adaptive sensorimotor network inspired by the anatomy and physiology of the cerebellum*. (pp. 301–348) Cambridge, MA: MIT Press.
- Kawano, K., Sasaki, M., & Yamashita, M. (1984). Response properties of neurons in posterior parietal cortex of monkey during visual-vestibular stimulation. I. Visual tracking neurons. *Journal of Neurophysiology*, 51(2), 340–351.
- Kawano, M., Shidara, Y., Watanabe, Y., & Yamane, S. (1994). Neural activity in cortical area MST of alert monkey during ocular following responses. *Journal of Neurophysiology*, 71(6), 2305–2324.
- Kawato, M. (1999). Internal models for motor control and trajectory planning. *Current Opinion in Neurobiology*, 9, 718–727.
- Keller, E. (1973). Accommodative vergence in the alert monkey. Motor unit analysis. *Visual Research*, 13, 1565–1575.
- Komatsu, H., & Wurtz, R. (1988a). Relation of cortical areas MT and MST to pursuit eye movements. I. Localization and visual properties of neurons. *Journal of Neurophysiology*, 60(2), 580–603.
- Komatsu, H., & Wurtz, R. (1988b). Relation of cortical areas MT and MST to pursuit eye movements. III. Interaction with full-field visual stimulation. *Journal of Neurophysiology*, 60(2), 621–644.
- Komatsu, H., & Wurtz, R. (1989). Modulation of pursuit eye movements by stimulation of cortical areas MT and MST. *Journal of Neurophysiology*, 62(1), 31–47.
- Krauzlis, R., & Lisberger, S. (1994). A model of visually-guided smooth pursuit eye movements based on behavioral observations. *Journal of Computational Neuroscience*, 1, 265–283.
- Kuroda, S., Schweighofer, S., & Kawato, M. (2001). Exploration and prediction of signal transduction pathways in cerebellar long-term depression by kinetic simulation. *Journal of Neuroscience*, 21(15), 5693–5702.
- Lisberger, S., & Movshon, J. (1999). Visual motion analysis for pursuit eye movements in area MT of macaque monkeys. *Journal of Neuroscience*, 19(6), 2224–2246.
- Ljung, L., & Soderstrom, T. (1986). *Theory and practice of recursive identification*. New York: MIT Press.
- MacAvoy, M., Gottlieb, J., & Bruce, C. (1991). Smooth-pursuit eye movement representation in the primate frontal eye field. *Cerebral Cortex*, 1(1), 95–102.
- Morris, E., & Lisberger, S. (1983). Signals used to maintain smooth pursuit eye movements in monkeys: Effects of small retinal position and velocity errors. *Society for Neuroscience Abstract*, 9, 866.
- Morris, E., & Lisberger, S. (1987). Different responses to small visual errors during initiation and maintenance of smooth-pursuit eye movements in monkeys. *Journal of Neurophysiology*, 58(6), 1351–1369.
- Newsome, W., Wurtz, R., & Komatsu, H. (1988). Relation of cortical areas MT and MST to pursuit eye movements. II. Differentiation of retinal from extraretinal inputs. *Journal of Neurophysiology*, 60(2), 604–620.
- Pavel, M. (1990). Predictive control of eye movement. In E. Kowler (Ed.), *Eye movements and their role in visual and cognitive processes* (pp. 71–114). Amsterdam: Elsevier.
- Pola, J., & Wyatt, H. (1997). Offset dynamics of human smooth pursuit eye movements: Effects of target presence and subject attention. *Visual Research*, 37(18), 2579–2595.
- Pouget, A., Zhang, K., Deneve, S., & Latham, P. (1998). Statistically efficient estimation using population coding. *Neural Computation*, 10, 373–401.
- Rao, R. (1999). An optimal estimation approach to visual perception and learning. *Visual Research*, 39, 1963–1989.
- Rao, R., & Ballard, D. (1999). Predictive coding in the visual cortex: A functional interpretation of some extra-classical receptive-field effects. *Nature Neuroscience*, 2, R87.
- Robinson, D., Gordon, J., & Gordon, S. (1986). A model of the smooth pursuit eye movement system. *Biological Cybernetics*, 55, 43–57.
- Sakata, H., Shibutani, H., & Kawano, K. (1983). Functional properties of visual tracking neurons in posterior parietal association cortex of monkey. *Journal of Neurophysiology*, 49(6), 1364–1380.
- Salinas, E., & Abbott, L. (1995). Transfer of coded information from sensory to motor networks. *Journal of Neuroscience*, 15(10), 6461–6474.
- Shidara, M., Kawano, K., Gomi, H., & Kawato, M. (1993). Inverse-dynamics model eye movement control by Purkinje cells in the cerebellum. *Nature*, 365(6441), 50–52.
- Song, S., & Abbott, L. (2001). Cortical development and remapping through spike timing-dependent plasticity. *Neuron*, 32, 339–350.
- Squatrito, S., & Maioli, M. (1997). Encoding of smooth pursuit direction and eye position by neurons of area MSTd of macaque monkey. *Journal of Neuroscience*, 17(10), 3847–3860.
- Stark, L., Vossius, G., & Young, L. (1962). Predictive control of eye tracking movements. *Institute of radio engineers trans in human factors and electronics*, 3, 52–57.
- Taguchi, S., Tabata, H., Shibata, T., Doya, K., Kawato, M. (2002). A model of smooth pursuit eye movements based on Bayes filter. In Technical report of IEICE, Vol. (NC2001-117), (pp. 79–86)
- Taguchi, S., Tabata, H., Shibata, T., & Kawato, M. (2004). Transformation from population codes to firing rate codes by learning: Neural representation of smooth pursuit eye movements. *Systems and Computers in Japan*, 35(6), 79–88.

- Takemura, A., Inoue, Y., Gomi, H., Kawato, M., & Kawano, K. (2001). Change in neuronal firing patterns in the process of motor command generation for the ocular following response. *Journal of Neurophysiology*, 86, 1750–1763.
- Takemura, A., Inoue, Y., Kawano, K., & Miles, F. (2001). Single-unit activity in cortical area MST associated with disparity-vergence eye movements: Evidence for population coding. *Journal of Neurophysiology*, 85(5), 2245–2266.
- Tanaka, K., Sugita, Y., Moriya, M., & Saito, H. (1993). Analysis of object motion in the ventral part of the medial superior temporal area of the macaque visual cortex. *Journal of Neurophysiology*, 69(1), 128–142.
- Tanaka, M., & Lisberger, S. (2001). Regulation of the gain of visually guided smooth pursuit eye movements by frontal cortex. *Nature*, 409, 191–194.
- Tian, J.-R., & Lynch, J. (1996). Corticocortical input to the smooth and saccadic eye movement subregions of the frontal eye field in cebus monkeys. *Journal of Neurophysiology*, 76(4), 2754–2771.
- Todorov, E. (2000). Direct cortical control of muscle activation in voluntary arm movements: A model. *Nature Neuroscience*, 3(4), 391–398.
- Wang, S.-H., Denk, W., & Häusser, M. (2000). Coincidence detection in single dendritic spines mediated by calcium release. *Nature Neuroscience*, 3(12), 1266–1273.
- Westheimer, G. (1954). Eye movement response to a horizontally moving visual stimulus. *American Medical Association. Archives of Ophthalmology*, 52, 932–941.
- Whittaker, S., & Eaholtz, G. (1982). Learning patterns of eye motion for foveal pursuit. *Investigative Ophthalmology & Visual Science*, 23(3), 393–397.
- Witney, A., Goodbody, S., & Wolpert, D. (2000). Learning and decay of prediction in object manipulation. *Journal of Neuroscience*, 20, 334–343.
- Yamamoto, K., Kobayashi, Y., Takemura, A., Kawano, K., & Kawato, M. (2000). A mathematical analysis of the characteristics of the system connecting the cerebellar ventral paraflocculus and extraculomotor nucleus of alert monkeys during upward ocular following responses. *Neuroscience Research*, 38, 425–435.
- Yamamoto, K., Kobayashi, Y., Takemura, A., Kawano, K., & Kawato, M. (2002). Computational studies on the acquisition and adaptation of ocular following responses based on the synaptic plasticity in the cerebellar cortex. *Journal of Neurophysiology*, 87(3), 1554–1571.
- Yasui, S., & Young, L. (1975). Eye movements during after-image tracking under sinusoidal and random vestibular stimulation. In G. Lennerstrand, & P. Bach-y Rita (Eds.), *Basic mechanisms of ocular motility and their clinical implication* (pp. 509–513). Oxford: Pergamon Press.
- Zemel, R., Dayan, P., & Pouget, A. (1998). Probabilistic interpretation of population codes. *Neural Computation*, 10, 403–430.